Guest Exchange Mechanism in the Clathrate Phase of Syndiotactic Polystyrene

Yukihiro Uda, Fumitoshi Kaneko,* and Tatsuya Kawaguchi

Department of Macromolecular Science, Graduate School of Science, Osaka University, Toyonaka, Osaka 560-0043, Japan

Received November 24, 2004; Revised Manuscript Received December 27, 2004

ABSTRACT: The guest exchange mechanism in the clathrate phase of syndiotactic polystyrene (sPS) was investigated by ATR−FTIR spectroscopy utilizing the selectivity of the sPS crystalline region about the conformation of 1,2-dichloroethane (DCE). 1,2-Dichloroethane (h-DCE) and its deuterated compound (d-DCE) were used as guests to analyze the sorption behavior of the sorbate molecules and the desorption behavior of the guest molecules stored in the crystalline region beforehand, simultaneously. The spectral changes on the exposure of an sPS film containing d-DCE to h-DCE vapor were followed, and the information about the guest exchange processes in both the crystalline and amorphous regions were obtained. In the earliest stage, the exchange occurred mainly in the amorphous region, while the exchange in the crystalline region proceeded gradually for a long time. On the basis of this finding, the diffusion coefficients of DCE molecules in the crystalline and amorphous regions were estimated.

Introduction

Since the synthesis of syndiotactic polystyrene (sPS) was reported,[1] a large number of works have focused on the complex polymorphic behavior of this polymer. At least four crystalline phases have been identified: α and β forms containing planar zigzag chains[2−7] and γ and δ forms containing helical chains of TTGG conformation.[8−11] The clathrate phase, in which guest molecules are located between sPS chains, can be obtained by solvent casting or sorption of suitable compounds into α, γ, and δ forms or amorphous sPS samples. The crystal structure of the clathrate phases including toluene and iodine have been described by Chatani et al.[8,9] De Rosa et al. have revealed the structure of the clathrate phase containing 1,2-dichloroethane.[10] The intensity and locations of the crystalline reflections in the X-ray diffraction patterns slightly change with the kind and amount of the included guest molecules. By conducting suitable extraction procedures on the clathrate sample, the nanoporous δ form in which guest molecules are removed from the cavities can be obtained.[11−13]

Among these crystalline phases, the nanoporous δ form has become of interest in recent years. Generally, the diffusion of low-molecular-weight compounds into the crystalline region of polymers is negligible. However, some solvent molecules are absorbed easily into the crystalline region of the nanoporous δ form even when at low vapor activities.[14,15] Some possible applications of this property of sPS such as chemical separations and sensing elements have been recently pointed out.[16−18]

As well as the preferential sorption of solvent vapor in the nanoporous δ form, the clathrate phase shows an interesting phenomenon. When a sample of the clathrate phase is exposed to a solvent vapor, the guest molecules stored in the cavities of the crystalline region are exchanged with the vapor molecules.[19−21] In the previous study, we followed the change in the amounts of sorbate and desorbate molecules as well as the conformational regularity of sPS chains by means of FTIR spectroscopy and clarified that the desorption of the guest molecules proceeded significantly faster on the guest exchange process than on the spontaneous desorption. However, the detailed mechanism of the guest exchange process has not been clarified yet.

sPS is a crystalline polymer. The sample of the clathrate phase consists of about 40% of crystalline region and the remaining amorphous region. The information about the behavior of the sorbate and desorbate molecules in the amorphous region is necessary for understanding the guest exchange mechanism. The IR data in our preceding study suggested that the guest exchange takes place in two steps: a rapid replacement of the sorbate with desorbate in the amorphous region in initial stage and a subsequent slow guest exchange in the crystalline region.[21] However, we could not obtain definite evidence of the above mechanism, since it was impossible to determine the ratio in real time at which the sorbate and desorbate molecules were distributed between the amorphous and crystalline regions.

For a more detailed description, we have investigated the guest exchange process using molecules that provide the information about their surroundings. 1,2-Dichloroethane whose characteristic conformational behavior in the clathrate phase was reported by Guerra et al. is just the one; despite nearly equal distribution between the trans and gauche conformers in the amorphous region, the trans conformer largely prevails in the crystalline region, and frequencies of some vibrational modes significantly depend on the conformation.[16,22,23] Furthermore, concomitant use of DCE and its deuteride makes it possible to determine the partition ratio in crystalline and amorphous regions for both sorbate and desorbate molecules.

This paper deals with the sorption and desorption behaviors of DCE and deuterated DCE on the guest exchange process, which has been studied by ATR−FTIR spectroscopy. On the basis of the time evolution of the partition ratio between the amorphous and crystalline regions, the guest exchange mechanism is described. In addition, the diffusion coefficients of DCE

* Corresponding author: e-mail toshi@chem.sci.osaka-u.ac.jp; Tel +81-6-6850-5453; Fax +81-6-6850-5288.

10.1021/ma047567a CCC: $30.25
Published on Web 03/22/2005

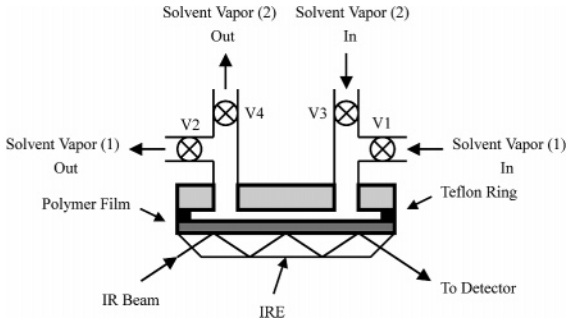

Figure 1. Schematic diagram of the ATR flow cell.

in the crystalline and amorphous regions are also discussed.

Experimental Section

Materials. Syndiotactic polystyrene (sPS) was kindly supplied by Idemitsu Petrochemical Co., Ltd. The weight-average molecular weight was M_w = 197 000 g/mol (M_w/M_n = 1.98). Chloroform and 1,2-dichloroethane (h-DCE) purchased from Nacalai Tesque and deuterated 1,2-dichloroethane-d_4 (d-DCE) purchased from Aldrich Chemical Co. were reagent grades and used without further purification.

Thin films of the clathrate phase including d-DCE as a guest were prepared by spin-coating from sPS/chloroform solution onto an internal reflection element (IRE) of KRS-5 followed by exposure to d-DCE vapor for 10 h. The thickness of the films was 2−3 μm, which was determined by comparing the absorbance of 1069 cm^{-1} band in transmission FTIR spectrum with that of the free-standing films of known thickness.

ATR−FTIR Measurements. ATR−FTIR spectra were taken with a BIO-RAD (Digilab) FTS-60A spectrometer equipped with a MCT detector at a resolution of 2 cm^{-1}. The IRE of KRS-5 with a 60° bevel was used. The apparatus used is illustrated in Figure 1. The inlet and outlet ports of the aluminum block are connected to Teflon tubing with Swagelok fittings. This system is composed of two pathways of solvent vapor, each of which consists of a solvent reservoir and a circulating pump. To ensure that the circulating air is saturated with solvent vapor in the system, air is bubbled through the solvent in the reservoir at least for 5 min before the beginning of exposure of the sample. The sealing between the inner surface of the block and the IRE is achieved by use of a Teflon ring.

The experimental procedure for guest exchange process is as follows. Until the start of the exposure to a h-DCE vapor, a specimen was kept in the vapor of d-DCE to prevent the desorption of d-DCE from the specimen, by setting valves V1 and V2 open and V3 and V4 closed. The exposure to h-DCE was started by opening V3 and V4 and closing V1 and V2 simultaneously. IR spectra were measured at 1 s intervals with four scans during the first 3 min of the experiment, and afterward acquisition time intervals and accumulation cycles increased gradually up to 5 h and 64 scans, respectively. All measurements were conducted at room temperature.

Data Analysis of ATR−FTIR Measurements. In ATR−FTIR spectroscopy the absorbance (A) of a film containing an absorbing species with concentration (C) can be expressed as

$$A = N\frac{n_2}{n_1}\frac{{E_0}^2\alpha}{\cos\theta}\int_0^L C(z)\exp(-2z/d_p)\,dz \tag{1}$$

where n_1 and n_2 are respectively the refractive indices of the IRE and the sample, θ is the incident angle, α is the absorption coefficient, N is the number of reflections in the IRE, E_0 is the amplitude of the evanescent wave at the interface between the IRE and the sample, z is the depth from the interface, d_p is the depth at which the amplitude of the evanescent wave decays to $1/e$ called the penetration depth, and L is the thickness of the sample.[24,25] The penetration depth is given by

$$d_p = \frac{\lambda}{2\pi n_1\sqrt{\sin^2\theta - (n_2/n_1)^2}} \tag{2}$$

where λ is the wavelength of infrared radiation. The absorbance ratio of trans to gauche conformer of DCE can be expressed as

$$\frac{A_t}{A_g} = \frac{\alpha_t}{\alpha_g}\frac{d_t}{d_g}\frac{C_t}{C_g}\frac{1-\exp(-2L/d_t)}{1-\exp(-2L/d_g)} \tag{3}$$

where the subscripts t and g refer to the trans and gauche conformers of DCE, and hence

$$\frac{C_g}{C_t} = \frac{\alpha_t}{\alpha_g}\frac{d_t}{d_g}\frac{A_g}{A_t}\frac{1-\exp(-2L/d_t)}{1-\exp(-2L/d_g)} \tag{4}$$

The mole fraction of the trans conformer, X_t, can be evaluated by

$$X_t = \frac{1}{1+\dfrac{C_g}{C_t}} \tag{5}$$

The ratio α_t/α_g has been evaluated from the value of X_t in the liquid phase reported in the literature (0.35 for h-DCE, 0.32 for d-DCE)[26,27] and from the absorbance ratio of the two analytical peaks in the ATR-FTIR spectrum of liquid h-DCE and d-DCE.

X-ray Diffraction Measurements. X-ray diffraction measurements were performed with a Rigaku RINT-2200 equipped with Cu Kα radiation (40 kV and 40 mA). The data were collected over the 2θ range from 5° to 40° at the scan speed of 0.5°/min with a step size of 0.05°.

Crystallite dimensions were calculated using the Scherrer equation given by

$$L_{hkl} = \frac{0.9\lambda}{\beta\cos\theta} \tag{6}$$

where L_{hkl} is the crystallite dimension perpendicular to the (hkl) plane, β is the half-width at half-maximum in radians for the diffraction peak, and θ is the half scattering angle.[28] The β values of the (010) and ($\bar{2}10$) diffraction peaks were evaluated by the Gaussian fitting. Silicon powder was used as a standard sample for evaluation of the instrumental broadening, for which we assumed Gaussian profiles.

Results and Discussion

Exchange Behavior of h-DCE and d-DCE. Figure 2 shows the ATR-FTIR spectral change of the clathrate phase containing d-DCE on exposure to h-DCE vapor. Just after the initiation of the exposure, the bands characteristic of trans and gauche conformers of h-DCE increased in intensity, and those of d-DCE decreased in intensity. Among these bands, the bands due to the CH_2 wagging mode of h-DCE and the CD_2 wagging mode of d-DCE were used for estimating the amounts of h-DCE and d-DCE in the crystalline and amorphous regions because they are very sensitive to the conformation and intense enough for quantitative analysis. The CH_2 wagging band appears at 1234 and 1285 cm^{-1} in the trans and gauche conformations of h-DCE, and the CD_2 wagging band appears at 938 and 1011 cm^{-1} in the trans and gauche conformations of d-DCE.[29] The gauche band of DCE derives mainly from the DCE molecules included in the amorphous region, while the trans band

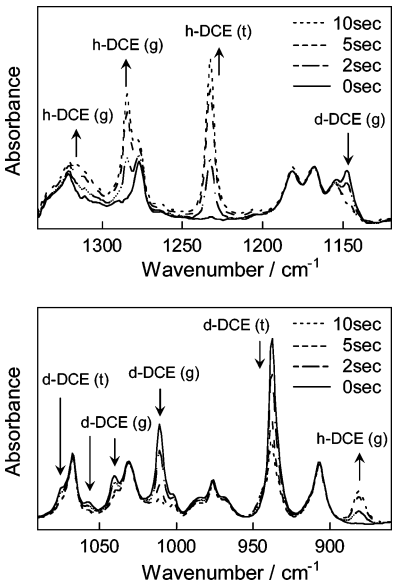

Figure 2. ATR−FTIR spectral change of the clathrate phase of sPS including d-DCE on the exposure to h-DCE vapor.

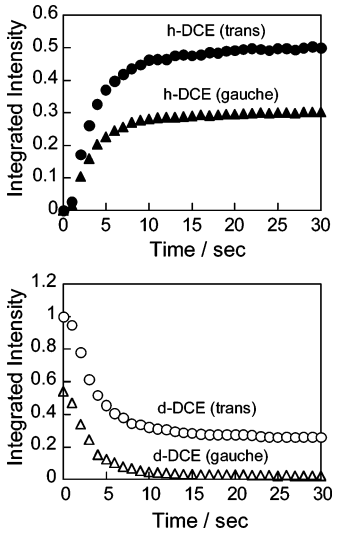

Figure 3. Absorbance of the trans and gauche bands of h-DCE and d-DCE plotted as a function of time.

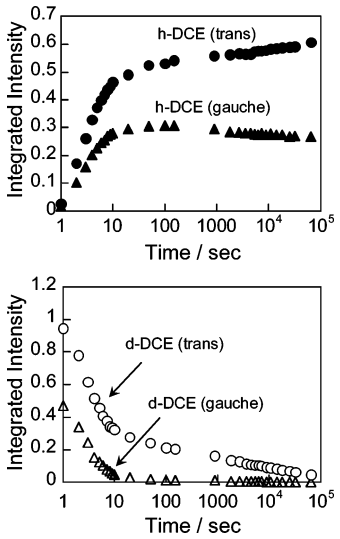

Figure 4. Absorbance of the trans and gauche bands of h-DCE and d-DCE plotted as a function of log time.

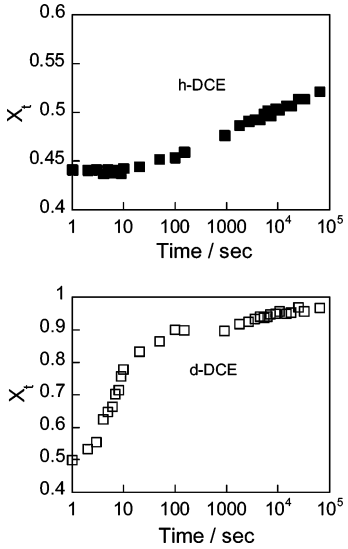

Figure 5. Fraction of trans conformer of h-DCE and d-DCE plotted as a function of time.

of DCE derives from the DCE molecules included in both the crystalline and amorphous regions.

The time dependence of the intensities of these bands is shown in Figure 3. Just after the start of the exposure of h-DCE, the gauche and trans bands of h-DCE began to increase in intensity, whereas those of d-DCE began to decrease. These results show that as h-DCE molecules penetrate into the sample, d-DCE molecules originally included in the sample were desorbed from the film. Although the intensity change of these bands slowed after about 5 s, the intensity change continued over a long time as shown in the plot of intensity vs log time in Figure 4. There was a clear difference in time dependence between the gauche and trans bands for both h-DCE and d-DCE. For h-DCE, the trans band gradually increased in intensity, whereas the gauche band once reached the maximum after about 100 s and then decreased in intensity slowly. For d-DCE, the intensity of the trans band became one-third of the value at the beginning in the first 10 s and decreased slowly, whereas the gauche band became almost faint in the first 10 s. The intensity ratio of trans to gauche band for d-DCE increased rapidly in the first 10 s, and then it gradually approached a constant value of 1:0.003. In the late stage, the trans and gauche bands of d-DCE gradually decreased in intensity without a large variation of the intensity ratio.

To show the conformational change of h-DCE and d-DCE more clearly, the time dependence of the molar fraction of the trans conformer, X_t, estimated using eq 5 is shown in Figure 5. The X_t value for d-DCE increased rapidly from 0.50 to 0.78 in the first 10 s and then gradually up to 0.96. This desorption behavior of d-DCE is analogous to the results of h-DCE desorption experiment under a nitrogen atmosphere reported by Musto et al.[22] On the contrary, the X_t value for h-DCE increased slowly from 0.44 with time. According to the results of Guerra et al., the amorphous region of sPS contains both the trans and gauche conformers to nearly the same extent, whereas the trans conformer prevails over the gauche conformer in the crystalline region of sPS; only several percent of DCE exist as the gauche conformer in the cavity.[16] Therefore, the changes in X_t suggest that the replacement from d-DCE to h-DCE took place primarily in the amorphous region in the first 10

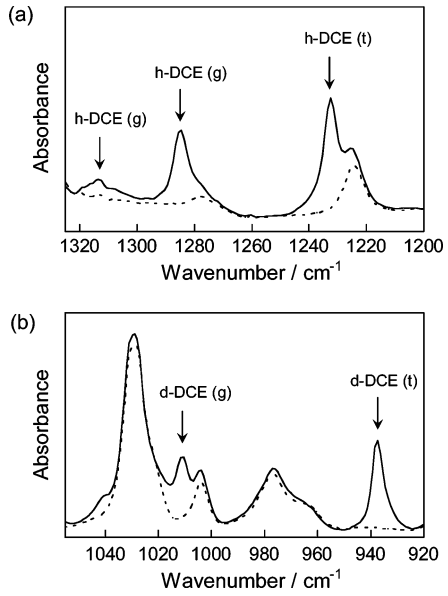

Figure 6. ATR−FTIR spectra of the solvent-free β form film (broken line) and the β form including solvent molecules (solid line): (a) h-DCE; (b) d-DCE.

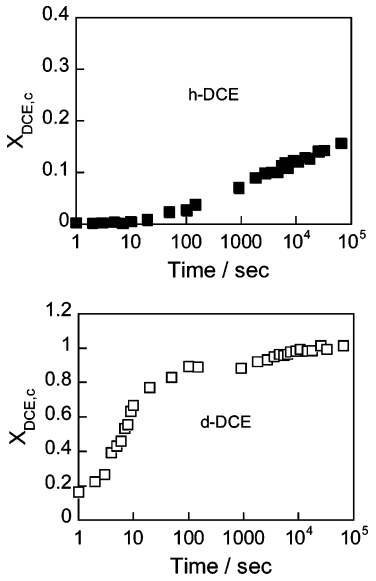

Figure 7. Fraction of DCE included in the crystalline region of the sample plotted as a function of time.

s, and then the slow guest exchange proceeded in the crystalline region.

In the final stage, the X_t value of 0.52 for h-DCE is rather small compared with that of 0.96 for d-DCE, which is due to the experimental conditions. The supply of the desorbate d-DCE to the sample was cut off at the inception of the measurement, and then the film was kept in a saturated vapor of the sorbate h-DCE. Therefore, the amorphous region was in equilibrium with the vapor in the final stage and contained a large amount of h-DCE molecules, about half of which took the gauche form. This leads to the increase of gauche conformer of h-DCE and reduces the ratio of the trans form for the whole h-DCE molecules in the film.

Fraction of DCE Included in the Crystalline Region. The fraction of DCE included in the crystalline region, $X_{\mathrm{DCE},c}$, can be estimated from the X_t values using the following relationship between $X_{\mathrm{DCE},c}$ and X_t reported by Daniel et al.[23]

$$X_{\mathrm{DCE},c} = \frac{1 - X_{t,a}}{X_{t,c} - X_{t,a}}\left(1 - \frac{1 - X_t}{1 - X_{t,a}}\right) \tag{7}$$

where X_t, $X_{t,c}$, and $X_{t,a}$ represent the fraction of trans conformer in the whole sample, crystalline region, and amorphous regions. The problem in applying this equation was the estimation of $X_{t,a}$. The direct evaluation of $X_{t,a}$ for the amorphous region of the clathrate sample was almost unrealistic, so we took the strategy that the value of $X_{t,a}$ obtained from the β form sample was adopted at the value of $X_{t,a}$ in the clathrate phase. Since both amorphous and crystalline region of the β form do not transform into the clathrate phase, the sorbate molecules can be considered to be in the amorphous region.[16,22]

Figure 6 shows the ATR-FTIR spectra of the β form containing h-DCE and d-DCE. The $X_{t,a}$ value was evaluated as 0.41 for d-DCE and 0.44 for h-DCE from the relative intensity of trans and gauche bands of DCE using eqs 4 and 5. The reported value of $X_{DCE,c}$ was in the range 0.94−1.0.[16,22] In this study, we obtained $X_{t,c}$ = 0.96 value by assuming $X_{\mathrm{DCE},c}$ for d-DCE in the final stage to be 1.0. Figure 7 shows the time dependence of $X_{\mathrm{DCE},c}$ for h-DCE and d-DCE. $X_{\mathrm{DCE},c}$ for h-DCE was nearly zero during the first 10 s, while $X_{\mathrm{DCE},c}$ for d-DCE started to increase immediately, implying that the guest exchange in the amorphous region is prevailing in this period. On the other hand, the value of $X_{\mathrm{DCE},c}$ for h-DCE increased after 100 s, suggesting that the guest exchange in the crystalline region dominantly proceeds in this stage. From the large difference in the time dependence of $X_{\mathrm{DCE},c}$ around 10 s, a two-step process can be deduced: the rapid guest exchange in the amorphous region and the gradual guest exchange in the crystalline region.

Estimation of Diffusion Coefficients As apparent from the desorption curve of d-DCE in Figure 4, the diffusion of d-DCE in the amorphous region is exceedingly faster than that in the crystalline region. For the first 5 s, the rate of desorption from the film is mainly determined by the desorption process of d-DCE from the amorphous region, whereas the desorption rate in the late stages is mainly determined by the desorption from the crystalline region. Using this property, we evaluated the diffusibility of d-DCE in the amorphous and crystalline regions as follows.

As for the desorption of d-DCE in the early stage, we can ignore the contribution of the desorption from the crystalline region. The diffusion coefficient of a desorbate can be estimated under the assumption of Fickian diffusion from the intensity change of a desorbate band with time in ATR-FTIR measurements using the following equation developed by Barbari et al.

$$\ln\left(\frac{A_t}{A_0}\right) = \ln\left(\frac{64\gamma^2 L^2}{\pi(16\gamma^2 L^2 + \pi^2)}\right) - \frac{D\pi^2}{4L^2}\,t \tag{8}$$

where A_0 and A_t are the infrared absorbance of the desorbate at time 0 and t, L is the film thickness, D is the diffusion coefficient, and γ is the reciprocal penetration depth given by[25]

$$\gamma = \frac{1}{d_p} = \frac{2n_1\pi\sqrt{\sin^2\theta - (n_1/n_2)^2}}{\lambda} \tag{9}$$

where n_1 and n_2 are the refractive indices of IRE and sample, λ is the wavelength of the IR radiation, and θ is the incident angle. Using this equation, D was estimated to be 3×10^{-8} cm^2/s from the slope in the plot of $\log(A_t/A_0)$ vs time using the data of the intensity change of the d-DCE gauche band for the first 3 s.

From the value of D, we evaluated the diffusion coefficient for amorphous region as follows. As for the diffusion of small molecules in the amorphous region, the existence of crystallites has a significant influence. Generally, the following two factors are considered: the geometrical impedance factor which accounts for the reduction in diffusion coefficient due to the necessity of molecules to bypass crystallites and the chain immobilization factor which takes into account the reduction in amorphous chain segment mobility due to the proximity of crystallites.[30] However, these factors are difficult to evaluate, and there is no settled protocol for the evaluation. So we employed the well-known Maxwell's formula which describes the diffusion in a heterogeneous material containing nonoverlapping spherical inclusions randomly placed throughout the material where these inclusions do not produce effects depending on their interference.[31] The equation is expressed simply as a function of the volume fraction of the dispersed phase:

$$\frac{D}{D_A} = \frac{2D_A + D_B - 2\phi(D_A - D_B)}{2D_A + D_B + \phi(D_A - D_B)} \tag{10}$$

where ϕ is the volume fraction of the dispersed phase, D is the effective or overall diffusion coefficient of molecules in the entire system, and D_A and D_B are the diffusion coefficients of molecules in the continuous and dispersed phases, respectively. In our system, D_A and D_B correspond to the diffusion coefficients of the amorphous and crystalline regions, D_a and D_c. In the early stage, the diffusion within crystallites can be ignored ($D_c = 0$), and the following simple equation is derived for the diffusion of molecules in a clathrate film.

$$\frac{D}{D_a} = \frac{2(1-\phi)}{2+\phi} \tag{11}$$

Using eq 11 and applying the value of crystallinity of the sample 0.4 to ϕ, the diffusion coefficient in the amorphous region D_a was estimated at 6×10^{-8} cm^2/s.

As for the d-DCE desorption from the crystalline region, we considered that the desorption rate from the crystalline region is the rate-determining step for the whole desorption process. Under this assumption, we evaluated the diffusion coefficient in the crystalline region D_c by considering the desorption from a crystallite of the average size. For this purpose, we need the average size and shape of crystallites and the direction in which solvent molecules diffuse.

It is difficult to investigate the direction of diffusion experimentally. Milano et al. and Tamai et al. calculated the diffusion coefficients of small molecules along each crystal axis of the nanoporous δ form by molecular dynamics simulation.[32,33] According to their results for various kinds of molecules at various temperatures, the diffusion coefficient does not depend strongly on the direction.

The crystallite size can be estimated from the line width of the X-ray diffraction peaks using the Scherrer equation.[28] Figure 8 shows the X-ray diffraction patterns

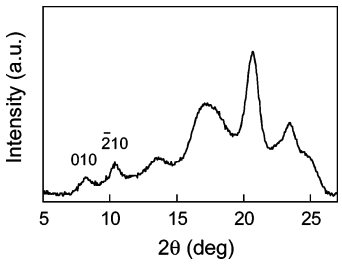

Figure 8. X-ray diffraction patterns of the clathrate phase including h-DCE as a guest.

of the clathrate phase including h-DCE as a guest. The crystallite sizes along the directions perpendicular to the (010) and ($\bar{2}$10) planes, L_{010} and $L_{\bar{2}10}$, were estimated to be 16 and 20 nm, respectively, using the diffraction peaks at $2\theta = 8.0°$ and 10.4°. The lamellar thickness of the clathrate phase was evaluated at 2.4 nm from a value of 5.9 nm for the lamellar thickness and crystallinity $X_c = 0.40$.[34] It is suggested that the lamellar thickness is relatively small compared to the lengths of the side of the basal plane, and most d-DCE molecules desorb through the lamellar surfaces.

Taking the above results into account, we have evaluated the diffusion coefficient based on the following assumptions; the anisotropy of the diffusion coefficient can be ignored, and the shape of the crystallite can be approximated by a flat rectangular parallelepiped with square basal planes. In this case, the time dependence of d-DCE's concentration is expressed as

$$\frac{C_t}{C_0} = \frac{512}{\pi^6}\sum_{p=0}^{\infty}\frac{1}{(2p+1)^2} \times \exp\left\{\frac{-D_c(2p+1)^2\pi^2 t}{{L_a}^2}\right\}\sum_{m=0}^{\infty}\frac{1}{(2m+1)^2} \times \exp\left\{\frac{-D_c(2m+1)^2\pi^2 t}{{L_a}^2}\right\}\sum_{n=0}^{\infty}\frac{1}{(2n+1)^2} \times \exp\left\{\frac{-D_c(2n+1)^2\pi^2 t}{{L_c}^2}\right\} \tag{12}$$

where C_0 and C_t are the concentrations at time 0 and t; and L_a and L_c are the lengths of the side of the basal plane and the lamella thickness.[35] Equation 12 can be rewritten for the late stage of the desorption as

$$\frac{C_t}{C_0} = \frac{512}{\pi^6}\exp\left\{-\pi^2 D_c t\left(\frac{2}{{L_a}^2} + \frac{1}{{L_c}^2}\right)\right\} \tag{13}$$

Since the infrared absorbance A is proportional to the concentration of d-DCE, a log A vs time plot gives a diffusion coefficient $D_c = 1 \times 10^{-19}$ cm^2/s using the values of $L_a = 18$ nm and $L_c = 2.4$ nm.

The obtained value of $D_a = 6 \times 10^{-8}$ cm^2/s for d-DCE is larger than that reported on the ordinary guest desorption,[36] and the value of $D_c = 1 \times 10^{-19}$ cm^2/s for d-DCE is smaller than that reported on the guest exchange process.[21] However, we should be careful when comparing diffusion coefficients obtained under different experimental conditions as suggested by Musto et al.[36] The diffusion of penetrant in the amorphous region is greatly influenced by the plasticizing effect. Therefore,

the D_a depends significantly on the kind and concentration of penetrant. The value of D_a obtained in this study is regarded as the value for the sufficiently swollen amorphous region, since the film was continuously exposed to saturated vapor of h-DCE. It is also expected that the D_c decreases with the increase of guest concentration in the crystalline region because a guest molecule occupying a cavity may act as an obstacle to the diffusion of other guest molecules. In this study, the guest concentration in the crystalline region had been kept high during the guest exchange process, which would be the cause of the very low value of D_c. The present result suggests that the relatively thin lamellar thickness of the clathrate phase is a crucial factor for the smooth guest exchange process.

Conclusions

Guest exchange behavior in the clathrate phase of sPS was analyzed in detail by ATR−FTIR spectroscopy. To follow the exchange processes in the crystalline and amorphous regions separately, we used h-DCE and d-DCE as sorbate and desorbate, which show greatly different conformational preferences between the amorphous and crystalline regions. It was clarified that the exchange between the sorbate and desorbate molecules takes place exclusively in the amorphous region for the first 5 s, and then slow guest exchange proceeds in the crystalline region. From the intensity change of its IR bands, a extremely different diffusibility of guest molecules between the amorphous and crystalline region was also demonstrated. On the basis of these experimental results, it was pointed out that a relatively thin lamellar thickness is a crucial factor for the smooth guest exchange behavior of the clathrate phase.

Acknowledgment. The authors thank Idemitsu Petrochemical Co., Ltd., for supplying the sPS samples. They also thank Mr. Masayoshi Nishiyama (Central Workshop, Osaka University) for his help in the ATR−FTIR measurement. The financial support of the Ogasawara Foundation for the Promotion of Science & Technology is also acknowledged. Y.U. expresses his special thanks for the Center of Excellence (21COE) Program "Creation of Integrated EcoChemistry of Osaka University".

References and Notes

(1) Ishihara, N.; Seimiya, T.; Kuramoto, M.; Uoi, M. *Macromolecules* **1986**, *19*, 2464.
(2) Greis, O.; Xu, Y.; Asano, T.; Petermann, J. *Polymer* **1989**, *30*, 590.
(3) De Rosa, C.; Guerra, G.; Petraccone, V.; Corradini, P. *Polym. J.* **1991**, *23*, 1435.
(4) De Rosa, C. *Macromolecules* **1996**, *29*, 8460.
(5) Cartier, L.; Okihara, T.; Lotz, B. *Macromolecules* **1998**, *31*, 3303.
(6) De Rosa, C.; Rapacciuolo, M.; Guerra, G.; Petraccone, V.; Corradini, P. *Polymer* **1992**, *33*, 1423.
(7) Chatani, Y.; Shimane, Y.; Ijitsu, T.; Yukinari, T. *Polymer* **1993**, *34*, 1625.
(8) Chatani, Y.; Shimane, Y.; Inagaki, T.; Ijitsu, T.; Yukinari, T.; Shikuma, H. *Polymer* **1993**, *34*, 1620.
(9) Chatani, Y.; Shimane, Y.; Inagaki, T.; Shikuma, H. *Polymer* **1993**, *34*, 4841.
(10) De Rosa, C.; Rizzo, P.; Ruiz de Ballesteros, O.; Petraccone, V.; Guerra, G. *Polymer* **1999**, *40*, 2103.
(11) De Rosa, C.; Guerra, G.; Petraccone, V.; Pirozzi, B. *Macromolecules* **1997**, *30*, 4147.
(12) Manfredi, C.; De Rosa, C.; Guerra, G.; Rapacciuolo, M.; Auriemma, F.; Corradini, P. *Macromol. Chem. Phys.* **1995**, *196*, 2795.
(13) Amutha Rani, D.; Yamamoto, Y.; Mohri, S.; Sivakumar, M.; Tsujita, Y.; Yoshimizu, H. *J. Polym. Sci., Part B: Polym. Phys.* **2003**, *41*, 269.
(14) Manfredi, C.; Del Nobile, M. A.; Mensitieri, G.; Guerra, G.; Rapacciuolo, M. *J. Polym. Sci., Part B: Polym. Phys.* **1997**, *35*, 133.
(15) Larobina, D.; Sanguigno, L.; Venditto, V.; Guerra, G.; Mensitieri, G. *Polymer* **2004**, *45*, 429.
(16) Guerra, G.; Manfredi, C.; Musto, P.; Tavone, S. *Macromolecules* **1998**, *31*, 1329.
(17) Guerra, G.; Milano, G.; Venditto, V.; Lofferedo, F.; Ruiz de Ballesteros, O.; Cavallo, L.; De Rosa, C. *Macromol. Symp.* **1999**, *138*, 131.
(18) Mensitieri, G.; Venditto, V.; Guerra, G. *Sens. Actuators B* **2003**, *92*, 255.
(19) Chatani, Y.; Shimane, Y.; Inoue, Y.; Inagaki, T.; Ishioka, T.; Ijitsu, T.; Yukinari, T. *Polymer* **1992**, *33*, 488.
(20) Yoshioka, A.; Tashiro, K. *Macromolecules* **2003**, *36*, 3593.
(21) Uda, Y.; Kaneko, F.; Kawaguchi, T. *Polymer* **2004**, *45*, 2221.
(22) Musto, P.; Manzari, M.; Guerra, G. *Macromolecules* **1999**, *32*, 2770.
(23) Daniel, C.; Guerra, G.; Musto, P. *Macromolecules* **2002**, *35*, 2243.
(24) Ohta, K.; Iwamoto, R. *Appl. Spectrosc.* **1985**, *39*, 418.
(25) Fieldson, G. T.; Barbari, T. A. *Polymer* **1993**, *34*, 1146.
(26) Tanabe, K. *Spectrochim. Acta* **1972**, *28A*, 407.
(27) Alvarez, M.; Bermejo, F. J.; Howells, W. S.; Chieux, P.; Enciso, E.; Alonso, J.; Garcia, N. *J. Chem. Phys.* **1989**, *91*, 3689.
(28) Alexander, L. E. *X-ray Diffraction Methods in Polymer Science*; Wiley-Interscience: New York, 1969.
(29) Mizushima, S.; Shimanouchi, T.; Harada, I.; Abe, Y.; Takeuchi, H. *Can. J. Phys.* **1975**, *53*, 2085.
(30) Michaels, A. S.; Bixler, H. J. *J. Polym. Sci.* **1961**, *50*, 413.
(31) Maxwell, J. C. *Treatise on Electricity and Magnetism*; Dover: New York, 1954.
(32) Milano, G.; Guerra, G.; Müller-Plathe, F. *Chem. Mater.* **2002**, *14*, 2977.
(33) Tamai, Y.; Fukuda, M. *Polymer* **2003**, *44*, 3279.
(34) Moyses, S.; Sonntag, P.; Spells, S. J.; Laveix, O. *Polymer* **1998**, *39*, 3537.
(35) Inthoff, W.; Zimen, K. E. *Acta Polytech.* **1956**, *206*, 16.
(36) Musto, P.; Mensitieri, G.; Cotugno, S.; Guerra, G.; Venditto, V. *Macromolecules* **2002**, *35*, 2296.

MA047567A